# A One-pass Extended Depth of Field Algorithm Based on the Over-complete Discrete Wavelet Transform

Andrew P. Bradley and Pascal C. Bamford

Cooperative Research Centre for Sensor Signal and Information Processing (CSSIP)
School of Information Technology and Electrical Engineering
The University of Queensland, St Lucia, QLD 4072, Australia.
{bradley|bamford}@itee.uq.edu.au

## Abstract

In this paper we describe an algorithm for extended depth of field (EDF) imaging based on the over-complete discrete wavelet transform (OCDWT). We extend previous approaches by describing a, potentially real-time, algorithm that produces the EDF image after a single pass through the 'stack' of focal plane images. In addition, we specifically study the effect of over-sampling on EDF reconstruction accuracy and show that a small degree of over-sampling considerably improves the quality of the EDF image.

**Keywords**: Extended depth of field microscopy, discrete wavelet transform, shift invariance

## 1 Introduction

Extended depth of field (EDF), or depth of focus, algorithms create a single image where all of the objects in that image are (apparently) in focus. These algorithms are used in many imaging applications, but are particularly useful in bright field microscopy where the high magnification lenses used result in an extremely narrow depth of field. Therefore, an image taken at any one focal position will only have a sub-set of the objects in focus.

Typically, the input to an EDF algorithm is a set (or 'stack') of images taken at various focal ($z$) positions: $s(x,y;z)$. An EDF algorithm then selects the most 'in focus' pixels from each image in the stack and creates a single EDF image: $p(x,y)$. This EDF image is then suitable for either visual or automated analysis as a substitute for the 3-dimensional image stack.

Algorithms based on the wavelet transform (WT) have been shown to offer promising results compared to methods based on more traditional focus metrics [7]. In their simplest form, they perform a WT on each image in the focal plane stack and then select the largest magnitude wavelet coefficient at each spatial location for each scale, $j$.

$$WT : s(x,y;z) \rightarrow \left\{c_j(n,m;z)\right\}_j$$

$$g_j(n,m) = c_j\left(n,m;\underset{z}{\operatorname{argmax}}\left|c_j(n,m;z)\right|\right).$$

The inverse WT of these largest amplitude wavelet coefficients is then the EDF image.

$$WT^{-1} : \left\{g_j(n,m)\right\}_j \rightarrow p(x,y).$$

While this simple approach is reasonably effective, it is common to enforce some form of spatial constraint on the coefficients selected, for example see [4] and [7], and to perform post-processing on the EDF image to reduce the effects of ringing and/or false colour artefacts [3].

In this paper we propose an extension to this previous work on wavelet EDF imaging by describing an algorithm that:

1. Only requires one-pass through the stack of focal plane images to both generate of the EDF image and to perform post-processing;
2. Utilises an over-sampled wavelet transform [2], where the amount of over-sampling, and hence memory and computation load, can be traded-off against reconstruction accuracy;
3. Utilises a simplified contextual constraint based on the maximum coefficient amplitude in a local neighbourhood across all three orientation sub-bands at the same wavelet decomposition level.

This algorithm is evaluated on a set of 100 cytological images where each object of interest (the cell nuclei) has been segmented at the 'best' focal plane by a human observer. In particular, we compare the results of the proposed method to those obtained using a complex wavelet transform [3] and clearly demonstrate the effect of varying the amount of over-sampling in the wavelet decomposition.

## 2 The EDF Algorithm

### 2.1 The Over-complete DWT

The wavelet transform (WT) has been shown to be an invaluable tool in signal processing applications such as data compression and fast computations [5]. However, the most commonly used implementation of the WT, the critically sampled DWT (often attributed to Mallat [5]), is shift variant. Therefore, the DWT is not optimal for applications such as extended depth of field imaging because small changes in input image alignment can produce significant changes in the EDF image. Previously proposed solutions to this problem have been to use over-sampled decompositions, such as the complex WT [3], or fully sampled decompositions, such as the continuous WT or the *à trous* algorithm [6].

In this paper we utilise a novel over-complete discrete wavelet transform (OCDWT) [2] which allows us to trade-off the computational efficiency and sparse representation inherent in the critically sampled DWT and the shift-invariance inherent in the fully sampled *à trous* algorithm. The OCDWT applies the Mallat algorithm to the first $M$ levels of an $L$-level decomposition and then applies the *à trous* algorithm to the remaining ($L - M$) levels [2]. The OCDWT algorithm can be viewed as an initial down-sampling of the signal prior to a fully sampled *à trous* decomposition. Alternatively, it be seen as a generalisation of the DWT, that produces the conventional DWT when $M = L$ and produces the fully sampled *à trous* algorithm when $M = 0$.

### 2.2 Wavelet Coefficient Selection

Previous wavelet EDF algorithms have demonstrated the need for both spatial and sub-band consistency checks to be performed as part of the wavelet coefficient selection [3]. Spatial consistency implies that coefficient selection should be based on a local neighbourhood around each wavelet coefficient, whilst sub-band consistency implies that coefficient selection should be based on all three sub-bands at each scale, $j$. Typically, spatial consistency is implemented by computing the variance [7], or maxima [4] over a 3x3 or 5x5 neighbourhood. We chose to select coefficients based on their magnitude, rather than variance, as large magnitude wavelet coefficients:

- Correspond to the sharp, high-contrast features in the image;
- Make the largest (energy) contribution to the reconstruction;
- Require no numerical computation to find.

In this way, we select the coefficients from plane $z$ that are maximal over the neighbourhood function, $n_\theta$, defined as the 3x3 neighbourhood around the coefficient $c_{j\theta}(m,n)$ in all (three) orientation sub-bands, $\theta$, at each scale, $j$.

$$g_{j\theta}(n,m) = c_{j\theta}\left(n,m;\underset{z}{\operatorname{argmax}}\left|n_\theta(m,n;z)\right|\right)$$

It should be noted that this proposed coefficient selection criteria can be calculated in one-pass, one focal plane at a time, thus making it suitable for real-time implementation. The method simply has to store the current maximum coefficient values, $\hat{g}_{j\theta}(n,m)$, and update this if the coefficients from the new focal plane, $c_j(n,m;z)$, produce a larger $|n_\theta|$. This avoids both the necessity of loading the complete stack of focal planes into memory at one time and the multi-pass processing implied by applying consistency checks to a *map* image of the selected z-planes (e.g., as in [7]). However, the proposed method is still capable of generating the final map image of selected $z$ planes for each coefficient and this can be used for topological visualisation.

### 2.3 Post-processing

A limitation of the post-processing proposed in [3] is that it requires a second pass through the image stack in order to be computed. Therefore, we have implemented a simplified post-processing step that can be estimated from the focal plane images during wavelet coefficient selection. It requires that the maximum and minimum pixel values in the focal plane stack are calculated for each spatial location.

$$q_{\min}(x,y) = \underset{z}{\operatorname{argmin}}\big(s(x,y;z)\big),$$
$$q_{\max}(x,y) = \underset{z}{\operatorname{argmax}}\big(s(x,y;z)\big).$$

The EDF image is then processed to ensure that its pixel values lie within the same range as those in the original image stack.

$$p(x,y) = \begin{cases} q_{\max}(x,y) & \text{if } p(x,y) > q_{\max}(x,y) \\ q_{\min}(x,y) & \text{if } p(x,y) < q_{\min}(x,y) \\ p(x,y) & \text{otherwise} \end{cases}.$$

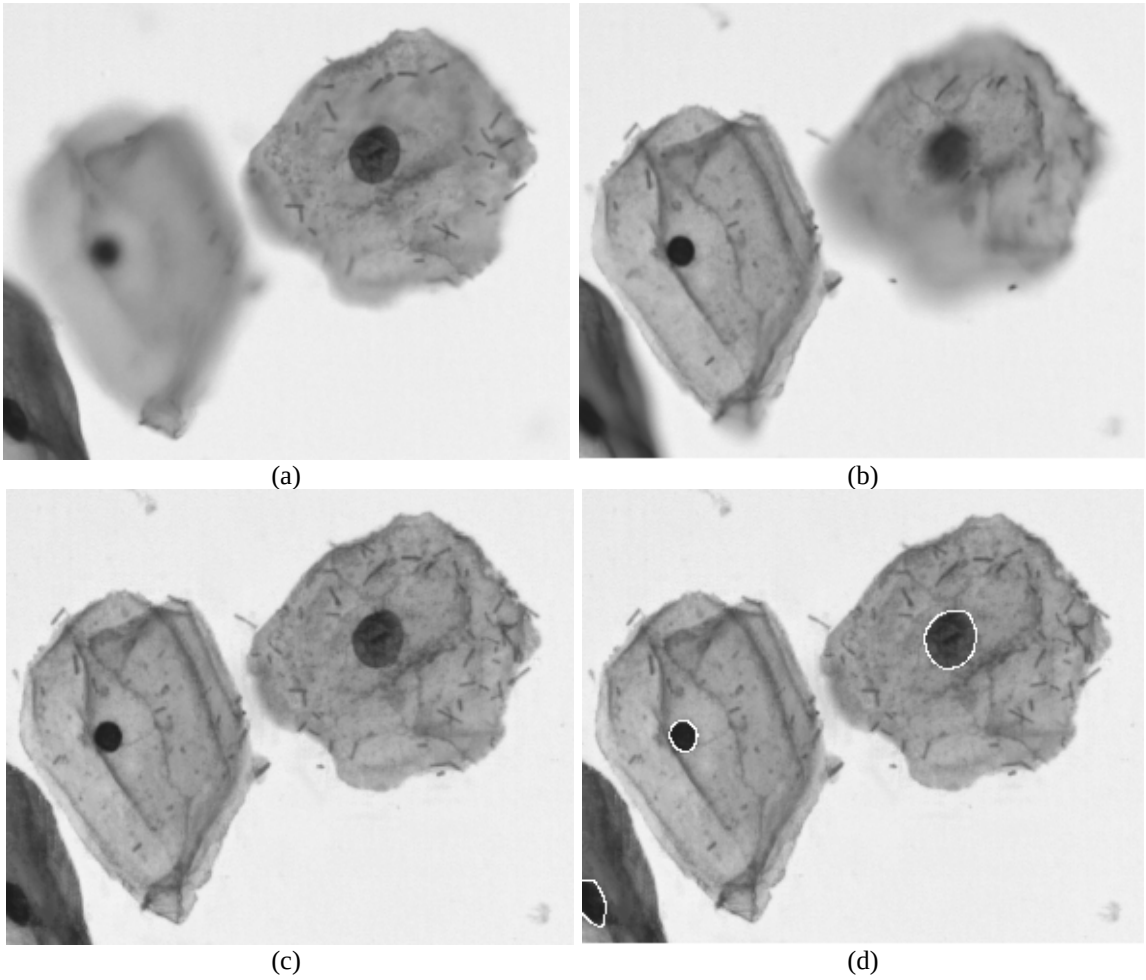

(a) (b)

(c) (d)

Figure 1 Example images from test dataset. (a) Image from a single focal plane showing two objects, one in focus and one out of focus; (b) same as (a) but taken at a focal plane where the object on the left is in focus; (c) example EDF image showing both objects synthetically in focus; (d) annotation of nucleus objects superimposed on the EDF image of (c).

## 3 Evaluation Methodology

Extended depth of field methods have previously been empirically evaluated using simulated data [3] or micrometer test slides [7]. Our objective was to use biological data in an application-driven evaluation protocol. We compared how closely the EDF images replicated images of selected objects of interest captured at their (different) optimal focal planes. This has application, for example, in scene segmentation where it may be more efficient to perform the segmentation on a single (EDF) image rather than on a number of images from different focal planes and then merging results.

### 3.1 Data Capture

A set of test images was captured from a biological sample consisting of Papanicolaou-stained cervical cells, at 40x magnification. One hundred non-overlapping fields of views (FOVs) were captured from a single slide. The specimen was approximately 20µm 'thick' in the *z*-dimension. The numerical aperture of the microscope objective used was 0.75 which gives a maximal depth of field of approximately 1µm. Therefore, for each FOV, a stack of twenty planes of focus were imaged at a separation in the *z*-dimension of 1µm.

### 3.2 Annotation

For each FOV, a number of image objects were selected for hand annotation. For each image object, the optimal focal plane for that object was selected by eye. Each object was then delineated by hand using a Wacom® PL400 pen-and-tablet and custom software written for the task. Both the delineated contour and the selected plane of focus were recorded for each object.

### Data Consistency Check

In order to verify that there was no systematic bias in the focal plane chosen for hand annotation, a simple consistency check was performed. For each annotated object, a focus measure was computed over the pixels corresponding to that object for all planes of focus.

Then, for each object, the plane number with maximal computed focus and human selected plane were compared. It was found that 98.4% of objects agreed to within one (±1) plane of focus (Figure 2). The focus measure used was the mean (Beucher's) gradient [1].

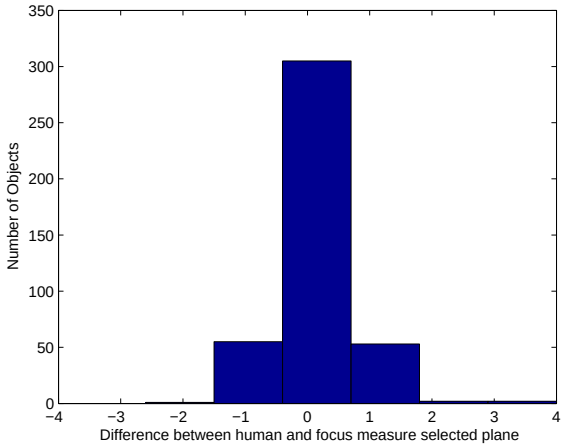


Figure 2. Histogram showing the correlation between the human and computed optimal focal plane for all image objects in the dataset.

### 3.3 Discrepancy Measure

In order to compare the EDF schemes under test, the mean squared error (MSE) between the EDF images and the best focal plane selected by eye was computed for each delineated object in each FOV. This compares how closely the original pixel intensities of each dataset object are reconstructed in the EDF images.

## 4 Results

The proposed method was first evaluated to observe the effect of over-sampling. That is, by varying the parameter $M$ that determines the number of levels of the DWT that are critically sampled. A plot of MSE versus $M$ for a ($L$ = 5) level transform is shown in Figure 3.

Next, the proposed method was evaluated with reference to a recently reported method [3], which has been implemented in publicly available software, making direct comparison with our results possible. To make the comparison as fair as possible we chose a mother wavelet with approximately the same support length and regularity as the complex Daubechies used in [3]: a 4$^{th}$ order, linear phase, bi-orthogonal spline [6]. In addition, we performed an ($L$ = 7) level decomposition, the default in [3], and again varied the amount of over-sampling by varying the parameter $M$.

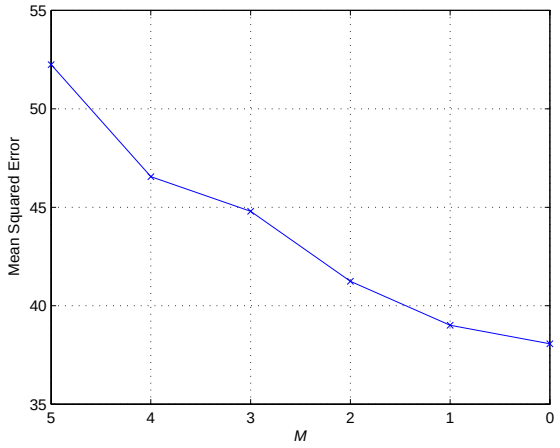


Figure 3. Plot of mean squared error (MSE) versus $M$, the number of critically sampled levels in the OCDWT.

Table 1 illustrates both the MSE and memory usage for the wavelet transform component of the various EDF algorithms (for an image with $N$ pixels). Memory usage for the CWT is twice that of the DWT (which is $N$, [6]) as the wavelet coefficients are now complex-valued. For a 2-dimensional, $L$ level, OCDWT, critically sampled to level $M$, memory requirements is given by [2]:

$$N + \frac{3(L-M)N}{2^M}.$$

Table 1. Mean square error (MSE) and memory usage for various ($L$=7) level wavelet transforms.

| Method | MSE | Memory |
|---|---|---|
| OCDWT ($M$ = 1) | 29.28 | 10$N$ |
| OCDWT ($M$ = 3) | 32.75 | 2.5$N$ |
| OCDWT ($M$ = 5) | 36.41 | 1.18$N$ |
| OCDWT ($M$ = 7) | 37.31 | $N$ |
| CWT [3] | 38.52 | 2$N$ |

## 5 Discussion

Figure 3 clearly shows the reduction in MSE of the EDF image as the amount of over-sampling in the WT is increased. It also illustrates that the shift variant nature of the (Mallat) DWT ($M$ = $L$ = 5) leads to poor MSE due to aliasing interfering with the coefficient selection. Although, the fully sampled *à trous* decomposition ($M$ = 0) has the minimum MSE, the decreasing gradient of the graph in Figure 3 shows that increasing the amount of over-sampling has a diminishing return in terms of reducing MSE. Therefore, an acceptable trade-off between memory usage and performance is obtained around $M$ = 2. These results confirm similar results already demonstrated in an edge detection scenario [2]. They also question whether the advantage of the CWT over the DWT is due to its complex-valued nature or the

fact that it is over-sampled compared to the critically-sampled DWT.

From Table 1 it can be seen that the proposed algorithm produces reduced MSE, for all values of *M*, compared to the previous EDF method based on the CWT. Table 1 also illustrates the memory requirements of the WT utilised in each of the methods and demonstrates that the approach utilised in the OCDWT is effective at reducing MSE for only modest increases in memory requirements.

The efficacies of the other aspects of the proposed method are illustrated by a significant rise in MSE when either no post-processing is performed (MSE increases by approximately 40) or when no contextual information is taken into account (MSE increases by approximately 8). These results are similar to those presented in [3].

## 6 Conclusions

We have proposed an algorithm for extended depth of field (EDF) imaging based on an over-complete discrete wavelet transform (OCDWT) and a novel sub-band neighbourhood coefficient selection strategy. The algorithm is efficient and potentially real-time as it can be implemented in one-pass, one focal plane at a time. The performance of the proposed technique was shown to be superior to a previously published technique on a set of 100 manually annotated cytology images. It was also demonstrated that by utilising the OCDWT it is possible to produce significantly improved EDF images at an over-sampling factor of around two.

## 7 References


[1] S. Beucher, "Segmentation Tools in Mathematical Morphology," *Proceedings of SPIE Conference on Image Algebra and Morphological Image Processing*, (1350) pp 70-84, San Diego, CA, 1990.

[2] A.P. Bradley, "Shift-invariance in the Discrete Wavelet Transform," *Proceedings of Digital Image Computing: Techniques and Applications* (DICTA'03), pp. 29-38, Sydney, Australia, December 2003.

[3] B. Forster, D. Van De Ville, J. Berent, D. Sage and M. Unser, "Extended Depth of Focus for Multi-Channel Microscopy Images: A Complex Wavelet Approach," *Proceedings of the 2004 IEEE International Symposium on Biomedical Imaging*, Arlington, VA, pp. 660-663, April 2004.

[4] H. Li, B.S. Manjuntah, S.K. Mitra, "Mutlisensor Image Fusion Using the Wavelet Transform," *Graphical Models and Image Processing*, Academic press, Vol. 57, No. 3, pp. 235-245, May 1995.

[5] S.G. Mallat, "A Theory for Multiresolution Signal Decomposition: the Wavelet Representation," *IEEE Transactions on Pattern Analysis and Machine Intelligence*, Vol. 2, pp. 674-693, 1989.

[6] S.G. Mallat, *A Wavelet Tour of Signal Processing*, 2nd Ed, Academic Press, 1999.

[7] A.G. Valdecasas, D. Marshall, J.M. Becerra, J.J. Terrero, "On Extended Depth of Focus Algorithms for Bright Field Microscopy," *Micron*, Pergamon, Vol. 32, pp. 559-569, 2001.